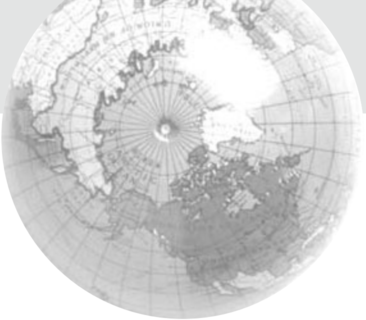

You will find the figures mentioned in this article in the German issue of ATZ 12|2007 beginning on page 1166.

Algorithmen zur Fahrspurprädiktion für Fahrerassistenzsysteme am Beispiel Adaptive Cruise Control

Path Prediction for Driver Assistance Systems exemplified on Adaptive Cruise Control

Specific driver assistance systems such as adaptive cruise control need a preferably precise path prediction of the driven car. That requires information about the curvature radius of the path as well as the sideslip angle of the own vehicle. Both are not available as measurement signals. The paper describes Volkswagen's algorithms of a model based path calculation using general available data.

Authors:
Yu Du, Arne Goldau and Stefan Wohlenberg

1 Introduction

Adaptive Cruise Control (ACC) is an essential improvement of a conventional speed control. Dependent on the traffic situations the ACC-system automatically adapts the speed of the own vehicle by active engine and brake interventions. **Figure 1** shows a typical scenario: The ACC-car is moving with a desired speed permanently observing a certain sector ahead and controlling the distance to a preceding vehicle. The ACC-car decelerates if the distance defined by a time gap can not be kept. When the preceding vehicle is leaving the lane the ACC-car is accelerating to the previous set driver demand.

ACC-Systems detect preceding vehicles moving in the same direction by means of range sensors, e.g. radar or laser. The nearest object on the future path of the ACC-car would be selected as the guiding one. Therefore a proper path prediction of the ACC-car is a precondition for the reliable selection of the relevant guiding vehicle.

2 Objective

Fundamental for a path prediction is reliable information about the current curvature radius and the sideslip angle which is defined as the angle between the vector of vehicle speed and the vector of vehicle longitudinal axis, **Figure 2**.

Figure 2 shows that the sideslip angle influences the result of path prediction. Corresponding to the direction of vehicle speed the centre of the circles has different positions, although the curvature radius is the same.

Therefore the task of path prediction contains the calculation of curvature radius and sideslip angle by means of available vehicle dynamic data. These data are:

- yaw velocity
- lateral acceleration
- steering angle
- wheel speed
- vehicle speed

In the following different approaches to calculate the curvature radius and the sideslip angle are described. They are outlined for driving conditions on motorways and highways. In these cases the vehicle movement can be characterized as steady state.

3 Algorithms of Path Prediction

The accuracy of path prediction depends on the quality of the available signals in the vehicle. A comprehensive consideration of all possibilities enables a choice of the best suitable algorithm dependent on the driving conditions.

3.1 Options of curvature radius calculation

At first different approaches to calculate the curvature radius are introduced.

3.1.1 Curvature radius calculation using yaw rate

According to **Figure 3** the curvature radius ρ is generally calculated as

$$\rho = \frac{v}{\dot{\psi} + \dot{\beta}} . \qquad \text{Eq. (1)}$$

There v denotes the vehicle velocity, $\dot{\psi}$ is the yaw rate and $\dot{\beta}$ describes the sideslip angle gradient of the vehicle. This relationship is valid for steady state as well as transient phases of a driving manoeuvre.

Steady state driving conditions result in $\dot{\beta} = 0$. Accordingly equation (1) reduces to

$$\rho = \frac{v}{\dot{\psi}} . \qquad \text{Eq. (2)}$$

This is not valid for transient manoeuvres. Neglect of sideslip angle gradient may lead to significant errors in curvature radius calculation.

3.1.2 Curvature Radius Calculation Using Lateral Acceleration

Another way to calculate the curvature radius is

$$\rho = \frac{v^2}{a} \text{, see Figure 3} \qquad \text{Eq. (3)}$$

There a denotes the centrifugal acceleration of the vehicle. It has to be considered that in a real vehicle the lateral acceleration a_y but not the centrifugal acceleration is measured.

The relationship between lateral acceleration and centrifugal acceleration is also shown in Figure 3. It is $a_y = a \cos\beta$. During ACC-relevant driving conditions the sideslip angle is small. Therefore the centrifugal acceleration in equation (3) can be substituted by the lateral acceleration.

Furthermore the lateral acceleration used above is always related to the vehicle centre of gravity. Accordingly the real position of the acceleration sensor in the vehicle has to be considered. That means:

$$a_y = a'_y - \dot{\psi}^2 l_y - \ddot{\psi} l_x \qquad \text{Eq. (4)}$$

Here a'_y is the sensor signal of lateral acceleration and the sensor position is described by the values l_x and l_y, Figure 3.

In steady state driving conditions there is no yaw acceleration, that means $\ddot{\psi} = 0$. If furthermore l_y is small, then the measured lateral acceleration is near to the lateral acceleration at the centre of gravity.

Resumed for steady state driving conditions the curvature radius can be calculated from the signal of lateral acceleration using equation (3).

3.1.3 Curvature Radius Calculation Using Wheel-speed Difference

During cornering the inside and the outside non-driven wheels have different speed. The wheel speed difference is influenced by the yaw velocity and finally by the curvature radius.

In **Figure 4** one can see the following kinematic relationships:

$$\omega_{HL} r = v \cos\beta - \dot{\psi} l_{HL} \sin\theta_{HL}, \qquad \text{Eq. (5)}$$

$$\omega_{HR} r = v \cos\beta - \dot{\psi} l_{HR} \sin\theta_{HR}. \qquad \text{Eq. (6)}$$

Subtraction of the equations results in $(\omega_{HR} - \omega_{HL}) r = \dot{\psi} (l_{HL} \sin\theta_{HL} + l_{HR} \sin\theta_{HR}) = \dot{\psi} B$, then

$$\dot{\psi} = \frac{(\omega_{HR} - \omega_{HL}) r}{B} . \qquad \text{Eq. (7)}$$

Applying equation (7) to equation (2) one obtains

$$\rho = \frac{vB}{(\omega_{HR} - \omega_{HL}) r} . \qquad \text{Eq. (8)}$$

If wheel slip occurs, e.g. during braking, equation (8) can not be used without modifications.

3.1.4 Curvature Radius Calculation Using Steering Wheel Angle

Riding a curve with a given radius and at a given velocity a certain steering wheel angle is needed. The correlation between the steering wheel angle and the curvature radius can be derived from a linear single-track model [2]:

$$\begin{bmatrix} \dot{\beta} \\ \ddot{\psi} \end{bmatrix} = \begin{bmatrix} \frac{-c_{\alpha V} - c_{\alpha H}}{mv} & \frac{-c_{\alpha V} l_V + c_{\alpha H} l_H}{mv^2} - 1 \\ \frac{-c_{\alpha V} l_V + c_{\alpha H} l_H}{J_Z} & \frac{-c_{\alpha V} l_V^2 - c_{\alpha H} l V_H^2}{J_Z v} \end{bmatrix} \begin{bmatrix} \beta \\ \dot{\psi} \end{bmatrix} + \begin{bmatrix} \frac{c_{\alpha V}}{mv} \\ \frac{c_{\alpha V} l_V}{J_Z} \end{bmatrix} \delta_V \qquad \text{Eq. (9)}$$

Thereby one term of the lateral acceleration $\dot{v}\beta$, which is induced by the longitudinal acceleration $\dot{v}$, was neglected. For the use case this term is comparatively small.

The single-track model represents the vehicle handling behaviour during ACC-relevant driving conditions very well. The parameters have the following meaning: m is the mass of the vehicle, J_Z denotes the moment of inertia related to vertical axis, $c_{\alpha V}$ and $c_{\alpha H}$ are the cornering stiffness values of the front and rear axle, l_V and l_H denote the position of centre of gravity in reference to the axles. Furthermore δ_V is the steering angle at the wheel which is connected with the steering wheel angle δ / i_S via the total steering gear ratio i_S. The relationship is $\delta_V = \delta / i_S$.

Under steady state conditions the sideslip angle and the yaw velocity are constant, i.e. $\dot{\beta} = 0$, $\ddot{\psi} = 0$. In that case the system of differential equations can be transferred to algebraic equations. Solving the equations for β and $\dot{\psi}$ results in

$$\dot{\psi} = \frac{c_{\alpha V} c_{\alpha H} v (l_V + l_H)}{c_{\alpha V} c_{\alpha H} (l_V + l_H)^2 + mv^2 (c_{\alpha H} l_H - c_{\alpha V} l_V)} \delta_V , \qquad \text{Eq. (10)}$$

$$\beta = \frac{c_{\alpha V} c_{\alpha H} l_H (l_V + l_H) - mv^2 c_{\alpha V} l_V}{c_{\alpha V} c_{\alpha H} (l_V + l_H)^2 + mv^2 (c_{\alpha H} l_H - c_{\alpha V} l_V)} \delta_V . \qquad \text{Eq. (11)}$$

Applying equation (10) to equation (2) one obtains:

$$\rho = \frac{c_{\alpha V} c_{\alpha H} v (l_V + l_H)^2 + mv^2 (c_{\alpha H} l_H - c_{\alpha V} l_V)}{c_{\alpha V} c_{\alpha H} (l_V + l_H)} \frac{1}{\delta_V} \qquad \text{Eq. (12)}$$

If $v \rightarrow 0$ then equation (12) reduces to

$$\rho = \frac{l_V + l_H}{\delta_V} = \frac{l}{\delta_V} . \qquad \text{Eq. (13)}$$

This equation exactly corresponds to the known equation that defines the Ackermann angle [3].

Equation (13) is only applicable at low speed. There the lateral forces and thus the wheel sideslip angle are negligible. Theoretically equation (12) could be used to calculate the curvature radius. But the practical application may be awkward, since this relationship is quite sensitive against changes of model parameters and inaccuracies in measurement signals.

3.2 Options of Sideslip Angle Calculation

In theory the sideslip angle can be determined directly with equation (11). As mentioned above the variability of vehicle parameters and the quality of measurement data restrict the use of equation (11). The calculation of sideslip angle is more reliable, if the signals of yaw rate and lateral acceleration are employed.

Considering the equations (10) and (11) the sideslip angle can be calculated from the yaw rate signal as follows

$$\beta = \left(\frac{l_H}{v} - \frac{m\, v\, l_V}{c_{\alpha H}(l_V + l_H)} \right) \dot{\psi} \; . \qquad \text{Eq. (14)}$$

Further in steady state there is

$$a_y \approx a = v\, \dot{\psi}, \qquad \text{Eq. (15)}$$

thus after a transformation of equation (14) we get the formula for the sideslip angle calculation using the lateral acceleration signal

$$\beta = \left(\frac{l_H}{v^2} - \frac{m l_V}{c_{\alpha H}(l_V + l_H)} \right) a_y \; . \qquad \text{Eq. (16)}$$

Moreover applying equation (7) to (14) the relationship between sideslip angle and wheel speed difference can be derived.

Finally for steady state driving conditions the relation between sideslip angle and curvature radius is given by

$$\beta = \left(l_H - \frac{m l_V\, v^2}{c_{\alpha H}(l_V + l_H)} \right) \frac{1}{\rho} \; . \qquad \text{Eq. (17)}$$

In the case that $v \rightarrow 0$ equation (17) reduces to:

$$\beta = \frac{l_H}{\rho} \qquad \text{Eq. (18)}$$

This equation represents the kinematic relation at low speed.

4 Practical Aspects

This chapter discusses the potentials and limits of path prdiction in practice.

4.1 Influence of Sideslip Angle on Path Prediction Quality

Motorways and highways are usually constructed from straight lines, circles with constant curvature and clothoides as junction curves. As an example a section of the German motorway A39 is shown in **Figure 5**. The curvature radius of the section is about 600 metres.

If a certain vehicle passes this section with different velocities the yaw velocity, the lateral acceleration, the sideslip angle, the steering angle and the wheel speed difference can be determined using the relations explained above. The resulting values are listed in the **Table**.

Table: Vehicle dynamic values at constant cornering

Velocity (km/h)	80	100	120	140	160	180	Equation
Yaw rate (°/s)	2.122	2.653	3.183	3.714	4.244	4.775	(2)
Lateral acceleration (m/s²)	0.823	1.286	1.852	2.521	3.292	4.167	(3)
Sideslip angle (°)	-0.078	-0.204	-0.359	-0.541	-0.752	-0.991	(17)
Steer angle at wheel (°)	0.326	0.370	0.424	0.487	0.560	0.643	(12)
Wheel speed difference (°/s)	10.823	13.528	16.234	18.939	21.645	24.351	(8)

The sideslip angle equals to -0.541° at a vehicle speed of 140 km/h, whereas the minus sign means that the vector of vehicle velocity is right from the vehicle longitudinal axis. In terms of path prediction accuracy neglect of the sideslip angle leads to a lateral deviation of 0.94 metres in a distance of 100 metres.

To clarify the correlation between the sideslip angle and the other physical values the angle is calculated using equation (17) at cornering with different velocities. The results are shown in **Figure 6**. The points on the vertical axis correspond to the kinematic behaviour. They are calculated from equation (18).

Figure 6 shows that all curves meet at a same point at zero-crossing. This point is defined by

$$\beta = \left(l_H - \frac{m l_V\, v^2}{c_{\alpha H}(l_V + l_H)} \right) \frac{1}{\rho} = 0.$$

At the corresponding velocity

$$v = \sqrt{\frac{c_{\alpha H} l_H (l_V + l_H)}{m l_V}} \; , \qquad \text{Eq. (19)}$$

which is only a function of vehicle parameters, the vehicle moves independent from the curvature radius without sideslip angle. At this velocity the sideslip angle changes its sign from minus to plus and vice versa.

Concerning the ACC-system only the driving situations with lateral acceleration below 4 m/s² are of interest. In figure 6 this area is shaded.

For a given time gap of 2.5 sec the ACC-relevant distance can be determined depending on the vehicle velocity. **Figure 7** shows errors of the path prediction at this distance if the sideslip angle is neglected. The higher the speed and the closer the curvature, the more is the error in path prediction, if sideslip angle is not considered.

4.2 Influence of Sensor Signal Errors on Path Prediction

Vehicle sensors work very different. Combining the available sensor information may lead to an appropriate complement and thus the reliability of the system increases.

In the following influences of sensor signal errors on the path prediction are discussed. To designate the offset of the calculated path in the ACC-relevant distance an auxiliary value σ has been introduced. This value is composed of σ_ρ and σ_β, **Figure 8**.

The offset σ_ρ results from the path curvature while σ_β is caused by the sideslip angle. The values can be calculated according to Figure 8 as follows

$$\sigma_\rho = s \cdot \arcsin \frac{s}{2\rho} \; , \qquad \text{Eq. (20)}$$

$$\sigma_\beta = s\beta. \qquad \text{Eq. (21)}$$

Here the ACC-relevant distance s is defined by the vehicle velocity v and the time gap t which is set by the driver.

$$s = v\, t \; . \qquad \text{Eq. (22)}$$

4.2.1 Influence of Yaw Rate Signal Errors

In terms of yaw rate signal the offset $\sigma = \sigma_\rho + \sigma_\beta$ can be expressed using equations (2), (14), (20), (21) and (22) as follows

$$\sigma = v\, t \cdot \arcsin \frac{t\dot{\psi}}{2} + \left(l_H - \frac{m l_V\, v^2}{c_{\alpha H}(l_V + l_H)} \right) t\dot{\psi}. \qquad \text{Eq. (23)}$$

If the measured yaw rate signal $\dot{\psi}'$ is different from the real value $\dot{\psi}$, e.g. $\dot{\psi}' = \dot{\psi} + \Delta\dot{\psi}$, then σ' and σ should be evaluated with equation (23) for $\dot{\psi}'$ and $\dot{\psi}$ respectively. Afterwards the variance $\Delta\sigma = \sigma' - \sigma$, which results from the error in the yaw rate signal $\Delta\dot{\psi}$, can be determined.

As an example **Figure 9**(a) shows the path prediction error due to a sensitivity error of 6.5 % in the yaw rate signal. Furthermore Figure 9(b) shows the path prediction error at an offset error of 0.35°/s in the yaw rate signal. The relevant areas (a_y < 4m/s²) are bold-dotted.

4.2.2 Influence of Lateral Acceleration Signal Errors

Taking equations (3), (16), (20), (21) and (22) into account the offset σ can be expressed with the lateral acceleration signal as

$$\sigma = vt \cdot \arcsin \frac{t a_y}{2v} + \left(\frac{l_H}{v} - \frac{m l_V v}{c_{\alpha H}(l_V + l_H)} \right) t a_y. \qquad (24)$$

Again the error in path prediction for different velocities and radii is plotted as a function of sensor errors. Now the sensitivity error of the lateral acceleration signal is 5.5 % and the offset is 0.15 m/s², **Figure 10**(a) and (b).

A comparison of the Figures 9(b) and 10(b) shows a contrary behaviour of the prediction error which is caused by the offset errors of the two sensors. This is easy to explain on the basis of the equation

$$\dot{\psi} = \frac{a_y}{v}$$

and accordingly

$$\Delta\dot{\psi} = \frac{\Delta a_y}{v} \; .$$

The equivalent error $\Delta\dot{\psi}$ due to error Δa_y decreases with increasing vehicle velocity. Therefore the lateral acceleration signal offers valuable information especially at high vehicle velocity.

One can see in the figures 9 and 10 that sensor errors allowed for vehicle dynamic control systems may induce unacceptable deviation for ACC-application. Especially the sensor offset errors may lead to serious problems because they are mostly significant higher as adopted in the examples. For this reason a reliable sensor calibration is of great importance.

5 Prospects

The introduced algorithms are designed for steady state driving conditions on motorways and highways.

The algorithms are not applicable for path prediction at transient driving manoeuvres. This limitation could be overcome if a dynamic vehicle model and adequate observers are introduced. Furthermore lateral road inclination highly influences the measured lateral acceleration, the wheel forces and consequently the sideslip angle. Algorithms which handle road inclination and transient driving manoeuvres will be specified in a separate article.

Vehicle parameters are of great importance in the presented algorithms. A few of them are not constant during driving. They can change slowly, e. g. due to abrasion, or fast due to loading or alternating road profiles. Adaptive algorithms are necessary to include these changes.

The calculations of the introduced methods base on information of the driven car. The extrapolated path is a good prediction if the car is moving on a road with a constant or moderate changing curvature. In other cases further information is essential for a reliable path prediction, e.g. information about preceding vehicles or standing objects. Evaluating this additional information the change of road curvature could be estimated, but it has to be differentiated whether cornering or lane change happens. Changes in azimuth angle and relative velocities which are interpreted in an appropriate time window could be used to assess the right manoeuvre.

Another source to get more information about the road is the navigation system. Because of technical constraints this is still in development.

Image processing enables object allocation as well as lane detection. This offers substantial information for complex traffic situations especially at low speed, e.g. stop and go.

References

[1] Winner, H. et. al.: Adaptive Fahrgeschwindigkeitsregelung ACC. Robert Bosch GmbH, Stuttgart, 2002

[2] Mitschke, M.: Dynamik der Kraftfahrzeuge, 4. Auflage. Springer-Verlag, Berlin, 1990

[3] Zomotor, A.: Fahrwerktechnik: Fahrverhalten, 2. Auflage. Vogel Verlag, Würzburg, 1991

[4] Kühne, M.: Einbindung von Navigationsdaten in Adaptive Cruise Control (ACC), Diplomarbeit, Audi AG / Universität Magdeburg. 2004

IMPRINT

ATZ WORLDWIDE

www.all4engineers.com

12|2007 · December 2007 · Volume 109
Vieweg Verlag | GWV Fachverlage GmbH
P.O. Box 15 46 · D-65173 Wiesbaden · Germany
Abraham-Lincoln-Straße 46 · D-65189 Wiesbaden · Germany

Managing Directors Dr. Ralf Birkelbach, Albrecht Schirmacher
Advertising Director Thomas Werner
Production Director Ingo Eichel
Sales Director Gabriel Göttlinger

EDITORS-IN-CHARGE

Dr.-Ing. E. h. Richard van Basshuysen
Wolfgang Siebenpfeiffer

EDITORIAL STAFF

Editor-in-Chief
Johannes Winterhagen (win)
Phone +49 611 7878-342 · Fax +49 611 7878-462
E-Mail: johannes.winterhagen@vieweg.de

Vice-Editor-in-Chief
Dipl.-Ing. Michael Reichenbach (rei)
Phone +49 611 7878-341 · Fax +49 611 7878-462
E-Mail: michael.reichenbach@vieweg.de

Chief-on-Duty
Kirsten Beckmann M. A. (kb)
Phone +49 611 7878-343 · Fax +49 611 7878-462
E-Mail: kirsten.beckmann@vieweg.de

Editors
Ruben Danisch (rd)
Phone +49 611 7878-393 · Fax +49 611 7878-462
E-Mail: ruben.danisch@vieweg.de

Dipl.-Ing. (FH) Moritz-York von Hohenthal (mvh)
Phone +49 611 7878-278 · Fax +49 611 7878-462
E-Mail: moritz.von.hohenthal@vieweg.de

Dipl.-Ing. Ulrich Knorra (kno)
Phone +49 611 78 78-314 · Fax +49 611 7878-462
E-Mail: ulrich.knorra@vieweg.de

Permanent Contributors
Christian Bartsch (cb), Prof. Dr.-Ing. Peter Boy (bo), Prof. Dr.-Ing. Stefan Breuer (sb), Jens Büchling (jb), Jörg Christoffel (jc), Prof. Dr.-Ing. Manfred Feiler (fe), Jürgen Grandel (gl), Erich Hoepke (ho), Thomas Jungmann (tj), Prof. Dr.-Ing. Fred Schäfer (fs), Roland Schedel (rs), Caterina Schröder (cs), Bettina Seehawer (bs)

Assistant
Martina Schraad
Phone +49 611 7878-244 · Fax +49 611 7878-462
E-Mail: atz-mtz@vieweg.de

Address
Postfach 15 46, D-65173 Wiesbaden,
Phone +49 611 7878-244 · Fax +49 611 7878-462

MARKETING | OFFPRINTS

Product Management Automedia
Sabrina Brokopp
Phone +49 611 7878-192 · Fax +49 611 7878-407
E-Mail: sabrina.brokopp@vieweg.de

Offprints
Martin Leopold
Phone +49 228 6907-87 · Fax +49 228-6907-88
E-Mail: leopold@medien-kontor.de

ADVERTISING | GWV MEDIA

Ad Manager
Nicole Kraus
Phone +49 611 7878-323 · Fax +49 611 7878-140
E-Mail: nicole.kraus@gwv-media.de

Key Account Manager
Elisabeth Maßfeller
Phone +49 611 7878-399 · Fax +49 611 7878-140
E-Mail: elisabeth.massfeller@gwv-media.de

Ad Sales
Susanne Ney
Phone +49 611 7878-222 · Fax +49 611 7878-140
E-Mail: susanne.ney@gwv-media.de

Display Ad Manager
Sandra Reisinger
Phone +49 611 7878-147 · Fax +49 611 7878-443
E-Mail: sandra.reisinger@gwv-media.de

Ad Prices
Price List No. 50

SUBSCRIPTIONS

Service
VVA-Zeitschriftenservice, Abt. D6 F6, ATZ
Postfach 77 77, 33310 Gütersloh
Renate Vies
Phone +49 5241 80-1692 · Fax +49 5241 80-9620
E-Mail: vieweg@abo-service.info

PRODUCTION | LAYOUT
Kerstin Gollarz
Phone +49 611 7878-173 · Fax +49 611 7878-464
E-Mail: kerstin.gollarz@gwv-fachverlage.de

PRINT | PROCESSING
Imprimerie Centrale Luxemburg. Printed in Europe.

SUBSCRIPTION CONDITIONS
The journal ATZ appears 11 times a year (with at least 5 additional special editions) at an annual subscription rate of 209 €. The price for an annual subscription including the English text supplement ATZ Worldwide is 259 €. Special rate for students on proof of status in the form of current registration certificate 81 €. Special rate for students including the English text supplement ATZ Worldwide 120 €. Special rate for VDI/VKS members on proof of status in the form of current member certificate 153 €. Special rate for studying VDI/ÖVK members on proof of status in the form of current registration and member certificate 45 €. Price per copy 23 €. All prices exclude mailing (annual subscription: inland 21 €; foreign countries 35 €; AirMail 109 €; annual subscription including the English text supplement ATZ Worldwide: inland 22 €; foreign countries 44 €; AirMail 119 €. Cancellation of subscriptions in writing at least six weeks before the end of the subscription year.

HINTS FOR AUTHORS
All manuscripts should be sent directly to the editors. By submitting photographs and drawings the sender releases the publishers from claims by third parties. Only works not yet published in Germany or abroad can generally be accepted for publication. The manuscripts must not be offered for publication to other journals simultaneously. In accepting the manuscript the publisher acquires the right to produce royalty-free offprints. The journal and all articles and figures are protected by copyright. Any utilisation beyond the strict limits of the copyright law without permission of the publisher is illegal. This applies particularly to duplications, translations, microfilming and storage and processing in electronic systems.